33rd Symposium on Naval Hydrodynamics
Osaka, Japan, October 18-23 2020

Support Vector Machine Learning Model of the Nonlinear Viscous Ship Roll Hydrodynamics

Y. Ma, D. F. H. Larson and P. D. Sclavounos
(Massachusetts Institute of Technology, Cambridge, MA, USA)

ABSTRACT

Support Vector Machine (SVM) learning algorithms have enjoyed rapid growth in recent years with applications in a wide range of disciplines, often with impressive results. The present paper introduces this machine learning technology to the field of marine hydrodynamics for the study of the nonlinear and viscous ship roll hydrodynamics. A key innovation of SVM kernel algorithms is that the nonlinear dependence of the dependent variable, e.g. a nonlinear load or response, upon a set of input variables, the "features", is embedded into the SVM kernel, the selection of which plays a key role in the performance of the algorithm. The kernel selection is discussed and its relation to the physics of the marine hydrodynamic flows under study in the present paper is addressed.

In this study, a series of computational fluid dynamics (CFD) simulations of the roll response of a rectangular barge with bilge keels are conducted and validated against experimental measurements, providing a baseline data set for the development of the SVM regression model. Using wave elevations and ship roll kinematics as features, an SVM regression model is trained and tested to predict the nonlinear hydrodynamic loads. Furthermore, using training response data from free decay tests and irregular wave simulations, the stochastic nature of ambient waves upon the nonlinear loads and roll responses is accounted for. The paper also compares and discusses different feature and kernel selections used in the model.

INTRODUCTION

The ship roll hydrodynamics problem is nonlinear and subjected to significant viscous effects arising from eddies shed from the hull, lifting effects for a ship advancing with forward speed and damping from bilge keels (Falzarano, et al. 2015). While other degrees of freedom motion can be predicted well by potential flow theory, the estimation of ship roll hydrodynamics remains a challenge. Numerous experiments and CFD simulations have been conducted to study the flow pattern towards the development of a model for ship roll hydrodynamics. Such experiments and CFD simulations are often combined with semi-empirical models for roll motion response prediction and for design purposes (Wassermann, et al., 2016; Irkal, et al., 2016; Kianejad, et al., 2019). The semi-empirical models are usually based on polynomial approximations which express the nonlinear roll damping and restoring forces in terms of the ship velocities and displacements.

However, as discussed by many researchers, the widely-used semi-empirical models with constant coefficients and linear or quadratic damping terms cannot fully capture the characteristics of ship roll hydrodynamics. Memory effects, the behavior for large roll amplitudes and the stochastic nature of irregular wave conditions need to be taken into account. Towards this objective, Bassler (2013) proposed a piecewise damping model to better predict large amplitude roll damping. However, we still lack a general model which takes into account all pertinent features of the nonlinear roll damping hydrodynamic problem. Therefore, the aim of the present study is to develop a better alternative to the traditional polynomial model.

Machine learning algorithms have enjoyed rapid growth in recent years with applications in a wide range of disciplines often with impressive results. Among various approaches, the Support Vector Machine (SVM) is one of the most widely used algorithms which leads to the representation of the physical quantity of interest as an explicit function of pertinent features (Christianini and Swane-Taylor, 2000; Sclavounos and Ma, 2018). Luo et al. (2016) have proposed the use of support vector machines for parameter identification in ship maneuvering models.

The essence of SVM algorithms is the use of kernels, instead of an explicit set of basis functions, in order to establish a compact functional relation between the output quantity being studied and a set of input explanatory variables, the features. Most SVM algorithms depend on two hyperparameters that control the regularization penalty and the mathematical form of the kernel. From the perspective of statistical learning theory, the kernel with the optimized hyperparameters determined during the training of the SVM algorithm, encodes the covariance structure between the features and forms the basis of the learning algorithm which relates the output quantity being modeled to the input features.

In the present study, the SVM model of the ship roll hydrodynamics problem proceeds along the following lines. A series of CFD simulations of a barge with bilge keels are conducted and validated. The results from these simulations serve as the training database and are then assumed to be an exact representation of the flow physics. An SVM regression model is established, using the ship roll motion kinematics and wave elevations over a time window of finite duration as the features. The size of the time window is selected to take into account memory effects and the stochastic nature of the ambient waves. The paper also compares and discusses alternative kernel selections used to build the SVM model.

LS-SVM REGRESSION MODEL

SVM regression uses a hypothesis space of basis functions in a high-dimensional feature space to represent the output variable, and is trained with an algorithm grounded in statistical learning theory. The least-squares support vector machine (LS-SVM) (Suykens and Vandewalle, 1999) minimizes a quadratic cost function and leads to the solution of a positive-definite linear system of equations which is explicit, as opposed to the convex quadratic programming problem of the classical SVM algorithm.

The LS-SVM regression assumes the following functional dependence between an output physical quantity y and the input explanatory K-dimensional vector of features $\boldsymbol{x} = [x_1, x_2, \ldots, x_K]^\intercal$,

$$y = \boldsymbol{w}^\intercal \boldsymbol{\phi}(\boldsymbol{x}) + b \tag{1}$$

The series expansion in (1) involves the unknown weight vector $\boldsymbol{w}$ and vector basis functions $\boldsymbol{\phi}(\boldsymbol{x})$. The constant b is the bias term. Given a sample of training data $\{(\boldsymbol{x}_i, y_i)\}_(i=1)^N$, LS-SVM determines the optimal weight vector and bias term by minimizing the cost function R,

$$\min_{\boldsymbol{w},\boldsymbol{e}} R(\boldsymbol{w}, \boldsymbol{e}) = \frac{1}{2}||\boldsymbol{w}||^2 + \gamma\frac{1}{2}||e||^2 \tag{2}$$

subject to the equality constraints,

$$y_i = \boldsymbol{w}^\intercal \boldsymbol{\phi}(\boldsymbol{x}_i) + b + e_i \quad \text{for } \; i = 1, 2, \ldots, N \tag{3}$$

where $||\cdot||$ denotes the Euclidean norm. The regularization parameter γ controls the trade-off between the bias and variance of the LS-SVM model. The error vector is $\boldsymbol{e} = [e_1, e_2, \ldots, e_N]^\intercal$.

Equations (2)-(3) form a standard optimization problem with equality constrains, for which the Lagrangian is,

$$L(\boldsymbol{w}, b, \boldsymbol{e}, \boldsymbol{\lambda}) = R(\boldsymbol{w}, \boldsymbol{e}) - \sum_{i=1}^{N} \lambda_i [\boldsymbol{w}^\intercal \boldsymbol{\phi}(\boldsymbol{x}_i) + b + e_i - y_i] \tag{4}$$

where λ_i are the Lagrange multipliers. According to the Karush-Kuhn-Tucker Theorem (Nocedal and Wright, 2006), the conditions of optimality are:

$$\begin{aligned} \frac{\partial L}{\partial \boldsymbol{w}} &= 0 \rightarrow \boldsymbol{w} = \sum_{i=1}^{N} \lambda_i \boldsymbol{\phi}(\boldsymbol{x}_i) \\ \frac{\partial L}{\partial b} &= 0 \rightarrow \sum_{i=1}^{N} \lambda_i = 0 \\ \frac{\partial L}{\partial e_i} &= 0 \rightarrow \lambda_i = \gamma e_i \\ \frac{\partial L}{\partial \lambda_i} &= 0 \rightarrow \boldsymbol{w}^\intercal \boldsymbol{\phi}(\boldsymbol{x}_i) + b + e_i - y_i = 0 \end{aligned} \tag{5}$$

The optimality conditions of (5) can be cast into a linear matrix equation,

$$\begin{bmatrix} 0 & \vec{\mathbf{1}}^\intercal \\ \vec{\mathbf{1}} & \boldsymbol{K} + \gamma^{-1}\boldsymbol{I} \end{bmatrix} \begin{bmatrix} b \\ \boldsymbol{\lambda} \end{bmatrix} = \begin{bmatrix} 0 \\ \boldsymbol{y} \end{bmatrix} \tag{6}$$

where $\vec{\mathbf{1}} = [1, \ldots, 1]^\intercal$. $\boldsymbol{I}$ is the identity matrix and $\boldsymbol{y} = [y_1, y_2, \ldots, y_N]^\intercal$. $\boldsymbol{K} = [k(\boldsymbol{x}_i, \boldsymbol{x}_j)]_{i,j=1}^{N}$ is called the kernel or Gram matrix defined by the inner product $k(\boldsymbol{x}_i, \boldsymbol{x}_j) = \boldsymbol{\phi}^\intercal(\boldsymbol{x}_i)\boldsymbol{\phi}(\boldsymbol{x}_j)$.

The LS-SVM regression model leads to a representation for the physical quantity being predicted in terms of the new feature vector $\boldsymbol{x}$, which takes the form

$$y(\boldsymbol{x}) = \sum_{i=1}^{N} \lambda_i k(\boldsymbol{x}, \boldsymbol{x}_i) + b \tag{7}$$

From equations (6)-(7), it can be seen that the basis functions $\boldsymbol{\phi}(\boldsymbol{x})$ do not need to be known explicitly. All that LS-SVM requires is the inner product of $\boldsymbol{\phi}(\boldsymbol{x})$, namely the kernel function $k(\boldsymbol{x}_i, \boldsymbol{x}_j)$. Widley used kernels include the linear, polynomial and Gaussian functions of the feature vectors. In the present study, the popular positive definite Gaussian kernel is used,

$$k(\boldsymbol{x}, \boldsymbol{z}) = \exp\left(\frac{-||\boldsymbol{x} - \boldsymbol{z}||^2}{\sigma^2}\right) \tag{8}$$

were $\boldsymbol{x}, \boldsymbol{z}$ are feature vectors corresponding to two samples, and $||\cdot||$ denotes the L2-norm of a vector. σ is a constant that controls the width of the Gaussian kernel and is evaluated by cross validation during the training of the SVM algorithm.

The selection of the Gaussian kernel and its popularity in a wide range of applications is not arbitrary. The connection between the kernel and the basis functions in kernelized machine learning algorithms such as the SVM, follows from Mercer's theorem (Christianini and Swane-Taylor, 2000), which states that for a positive definite kernel,

$$\begin{aligned} &\iint\limits_{X} k(\boldsymbol{x}, \boldsymbol{z})\, \phi_j(\boldsymbol{z})\ \mathrm{d}\boldsymbol{z} = \mu_j \phi_j \\ &k(\boldsymbol{x}, \boldsymbol{z}) = \sum_{j=1}^{\infty} \mu_j \phi_j(\boldsymbol{x})\, \phi_j(\boldsymbol{z}) \end{aligned} \tag{9}$$

For the Gaussian kernel, the solution of (9) is available in closed form in any number of dimensions. Consider the multi-dimensional Gaussian kernel assuming K-dimensional features. The explicit solution of (9) takes the form:

$$\begin{aligned} k(\boldsymbol{x}, \boldsymbol{z}) =& \exp\Big[-\varepsilon_1^2 (x_1 - z_1)^2 - \varepsilon_2^2 (x_2 - z_2)^2 - \dots \\ & \qquad -\varepsilon_k^2 (x_k - z_k)^2\Big] \\ =& \sum_{k \in N^K} \mu_k \phi_k(\boldsymbol{x})\, \phi(\boldsymbol{z}) \end{aligned} \tag{10}$$

Where, $\varepsilon_k^2 = 1/\sigma_k^2$, and σ_k refers to the constant determining the scale or variance of the k-th feature of the Gaussian kernel. The cross-correlation of the features may be assumed to vanish following a Principal Components Analysis or singular value decomposition of the covariance matrix of the input feature dataset (Bishop, 2006). The eigenvalues μ_k and eigenfunctions ϕ_k in (10) are available in closed form. Fasshauer and McCourt (2012) present the details of the underlying mathematical derivation.

The basis functions $\phi_j(x)$ are the generalized Hermite functions which are orthogonal over the entire real axis and are known to be a robust basis set for the representation of a wide range of smooth signals. The formulation of (10) allows the selection of different shape parameters σ_k for different space dimensions (i.e. the kernel k may be anisotropic). Alternatively, they may be assumed to be equal (i.e. k is spherically isotropic) as is the case in equation (8).

Another commonly used kernel is the polynomial kernel, which takes the form of

$$k(\boldsymbol{x}, \boldsymbol{z}) = (\boldsymbol{x}^{\mathsf{T}} \boldsymbol{z} + s)^d \tag{11}$$

where, s is the bias term and d is the degree of the polynomial kernel, which may be a non-integer real number.

On closer inspection of Eq. (10), it may be shown that the polynomial kernel is equivalent to an expansion of the Gaussian kernel into a Taylor series for small values of the inverse scales ε_k (Fasshauer and McCourt, 2012). In this study, the Gaussian kernel is selected for the SVM regression model due to its proven generalization capabilities. An SVM model with linear kernel ($d = 1$, $s = 0$ in Eq. (11)) is also developed in the present paper, viewed as the leading-order linear approximation of the more general Gaussian kernel, which behaves as an equivalent linearization when included in the linear frequency-domain roll transfer function.

CFD SIMULATIONS

In order to develop the SVM regression model for the ship roll hydrodynamics problem, a baseline dataset is needed for training and validation process. Due to free surface nonlinearities and viscous flow separation physics that dominate the ship roll motion problem, models based on potential flow theory are not adequate. Therefore, besides model tests, numerical simulations of the ship roll motions are conducted using the Siemens STAR-CCM+ solver. In this study, a barge in model scale is modeled using a 2D CFD solver which simulates the Reynolds-Averaged Navier-Stokes equations (Siemens, 2019).

The prototype ship dimension in model scale of 1/100 has a beam of 300 mm and a draft 120 mm, and was tested in a flume in the Department of Ocean Engineering, IIT Madras (Irkal, et al., 2014; Irkal, et al., 2016). A series of CFD simulations were carried out and used as the database for the training of the SVM regression model. The inertia and hydrostatic properties of the ship model and bilge keel dimensions are summarized in Table 1.

Table 1: Particulars for ship model with bilge keels

Draft	0.12 m
Displacement	20.88 kg
Roll Moment of Inertia (I)	0.2244 kg-m^2
Center of gravity from keel (KG)	0.08 m
Bilge keel width	10.0 mm
Bilge keel angle to horizontal	45°

The CFD hull model is a 2D section with beam equal to 1/20 of the ship length and one layer of mesh points in the longitudinal direction. Hexahedral mesh elements of varying resolution are used and mesh refinement is carried out in the vicinity of the bilge keels as well as on the free surface. An Eulerian multi-phase volume of fluid model is used to simulate and accurately capture free surface effects. The Reynolds stress is resolved using the k-ω SST turbulence model (Siemens, 2019). The computational domain is modeled by the overset mesh technique. The sketch of the simulation domain and mesh visualization is shown in Figure 1.

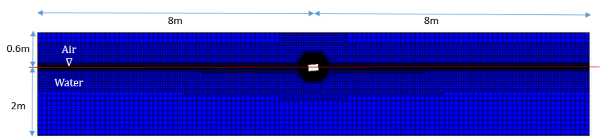

(a) Simulation domain

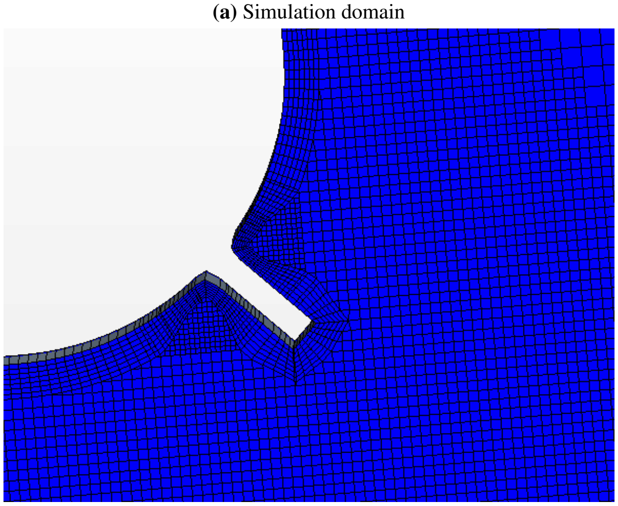

(b) Mesh refinement around the bilge keels

Figure 1: Mesh of the CFD domain

To validate the CFD simulations for subsequent use to train the SVM regression model, the single degree of freedom (DOF) ship roll motion is simulated under three different scenarios: a) free decay test in calm water, b) ship roll motion excited by regular waves with different wave frequencies, and c) ship roll motion in an irregular seastate.

Figure 2 illustrates the comparison of results between the current CFD simulations and the experiments (Irkal, et al., 2014; Irkal, et al., 2016) for the free decay test and the motion response under different regular wave conditions. The initial angle of the free decay test was set to 20 degrees. Five regular wave cases that covered the major excitation frequencies were simulated with the same wave height $H = 3$cm in model scale. The five different regular wave periods were 0.75s, 1s, 1.125s, 1.25s and 1.5s.

The good agreement between the CFD simulations and experiments for the free decay test and motion responses in regular waves (Figure 2) indicate that the refined mesh around the ship hull and in the vicinity of the bilge keels is sufficiently dense to capture the viscous separated flow physics. The response amplitude operator (RAO) in Figure 2 is defined as the ratio between the amplitude of ship roll displacement and the amplitude of the incident wave.

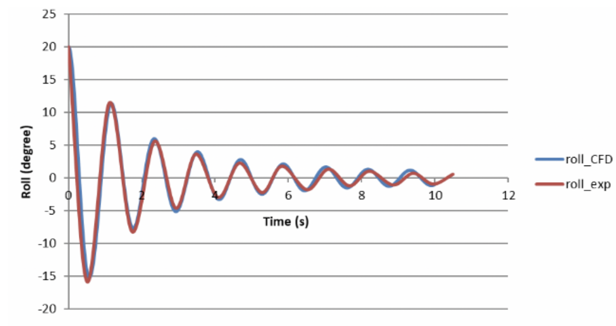

(a) Free decay test

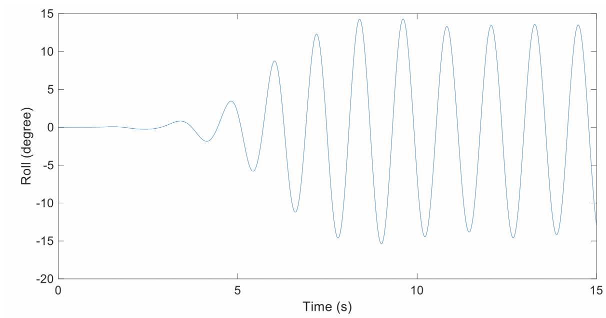

(b) Simulated ship roll response in a regular wave with period 1.2s and wave height 3cm

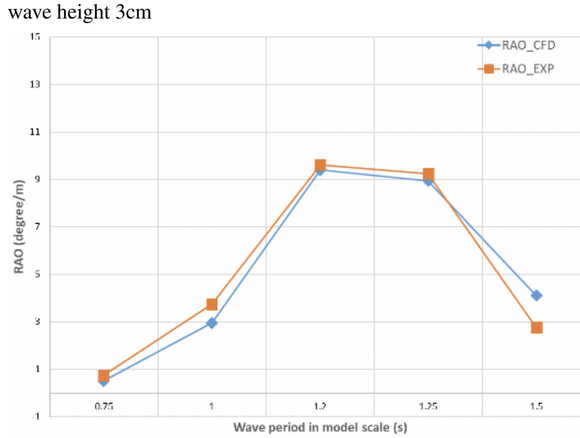

(c) Motion response amplitude operator (RAO) in regular waves

Figure 2: Validation of the CFD simulations against wave tank tests.

The single DOF ship roll motion was also simulated in an irregular sea state. The data in the following sections may be converted to full scale by using the scale ratio 1/100. The JONSWAP spectrum (Siemens,

2019) is used in this study to create a simulation of the irregular waves. The simulated sea state has a significant wave height (Hs) 6m and a modal wave period (Tp) 11.3s.

Although experimental results under irregular wave conditions are not available, Figure 3 shows the simulation of irregular waves in the absence of the ship. The simulated spectrum is well matched with the target one, indicating that the refined mesh employed around the free surface and the time step used in the simulations are sufficient to capture the free surface dynamics. Therefore, given the good performance of the CFD simulations for the free decay, regular and irregular wave tests, it is assumed that the CFD simulations of the ship roll hydrodynamics in irregular waves form an accurate database for the training of the SVM regression model. Figure 4 shows the simulated ship roll motion under irregular waves. The overall full scale simulation time is 3600s (1 hour), sufficiently long in order to evaluate statistically reliable moments.

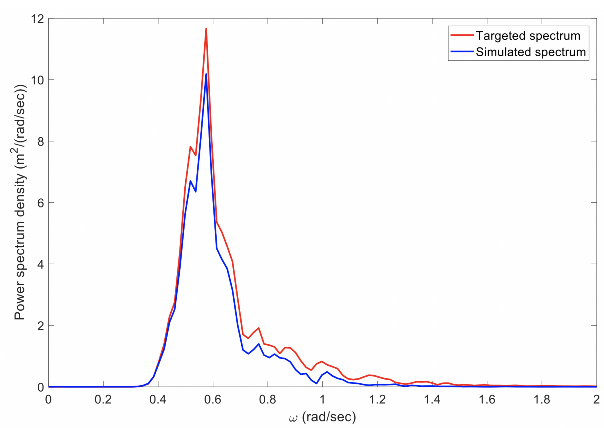

Figure 3: Validation of the irregular wave spectrum

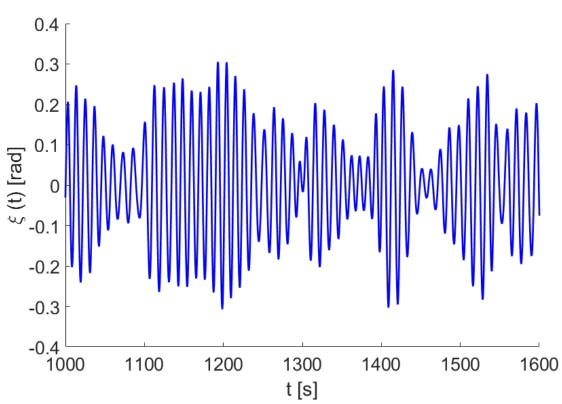

Figure 4: Segment of a 1-hour simulated ship roll response record under the irregular wave condition of $H_s = 6$m, $T_p = 11.3$s at full scale

SHIP ROLL HYDRODYNAMICS MODELING VIA LS-SVM REGRESSION USING FREE DECAY TEST DATA

For the free decay test, the 1-DOF equation of the ship roll motion can be expressed as

$$I\ddot{\xi}(t) = F_h\left(\xi(\tau), \dot{\xi}(\tau), \ddot{\xi}(\tau)\right) \tag{12}$$

where I is the moment of inertia of the ship hull structure. The overall hydrodynamic moment is F_h, which includes contributions from restoring, added mass and damping forces. $\xi(\tau), \dot{\xi}(\tau), \ddot{\xi}(\tau)$, are the past records of the ship roll displacement, velocity and acceleration, respectively, taking into account the memory effect. τ is a dummy variable representing the past time steps.

The overall hydrodynamic moment can be decomposed into several components using linear potential flow theory:

$$F_h(t) = -A_\infty\ddot{\xi}(t) - C\xi(t) + F_{h,r}(t) \tag{13}$$

where A_∞ is the infinite frequency added mass and C is the linear hydrostatic restoring coefficient. The components contributed by the fluid inertia and wave damping, viscous damping and nonlinear restoring force are all included in the term $F_{h,r}(t)$. $F_h(t)$ is the overall hydrodynamic moment derived from the integration of the pressure and stress from the CFD solver, and infinite-frequency added mass and linear hydrostatic restoring terms are simple functions of the ship hull geometry. $F_{h,r}(t)$ may therefore be cast in the form:

$$F_{h,r}(t) = F_h(t) + A_\infty\ddot{\xi}(t) + C\xi(t) \tag{14}$$

The features that $F_{h,r}(t)$ depends upon are the past records of the ship kinematics, which are available from the CFD simulations. Therefore, in the context of the LS-SVM model given by Eqs. (2)-(7), the training and test data samples $\{\boldsymbol{x}_i, y_i\}$ are defined as follows: $\boldsymbol{x}_i = \left[\xi_{t_i}, \xi_{t_{i-1}}, \ldots, \xi_{t_{i-d}}, \dot{\xi}_{t_i}, \dot{\xi}_{t_{i-1}}, \ldots, \dot{\xi}_{t_{i-d}}, \ddot{\xi}_{t_i}, \ddot{\xi}_{t_{i-1}}, \ldots, \ddot{\xi}_{t_{i-d}}\right]$, and $y_i = F_{h,r}(t_i)$. d is the duration of the past record, which takes into account memory effects.

The original sampling time step of the CFD simulations is 0.01 seconds in full scale. The duration of the past record that takes into account memory effect is set to 8 seconds. Therefore, in order to keep the dimensions of the features reasonable, the CFD simulated data are resampled at a time step 0.5s. The total number of samples generated in the free decay test is 1000, with 500 randomly selected samples used for training and the remaining 500 samples used for testing. The hyper-parameters, including the Gaussian kernel width and the regularization parameter, are optimized using

10-fold cross-validation during the SVM training process. The results of the training and testing are shown in Figure 5, where the radial basis function (RBF) kernel marked in the legends refers to the Gaussian kernel.

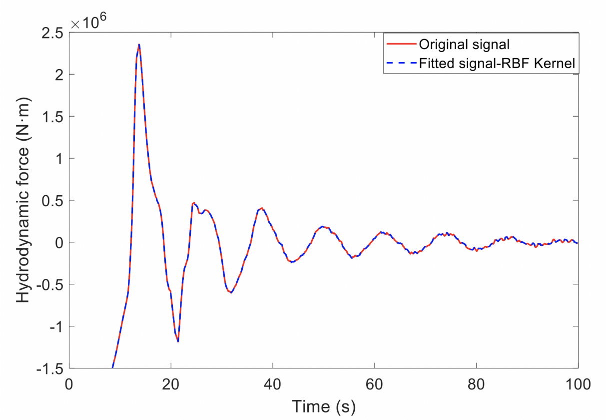

(a) Training data set

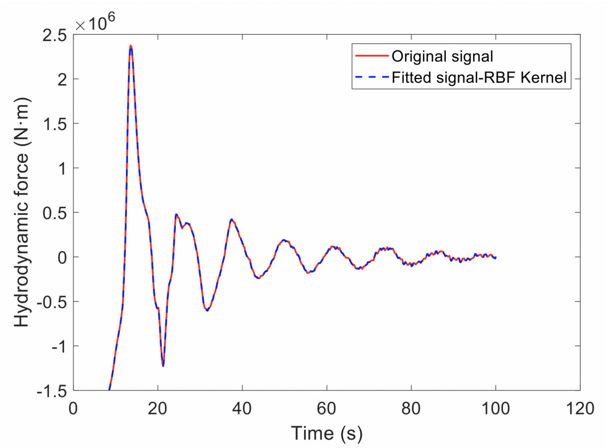

(b) Test data set

Figure 5: Hydrodynamic force prediction results using a Gaussian kernel for free roll decay

From these results, the SVM regression model may be seen to be able to capture the nonlinear mapping between the ship roll kinematics and the corresponding hydrodynamic forces in calm water conditions.

SHIP ROLL HYDRODYNAMICS MODELING VIA LS-SVM REGRESSION USING IRREGULAR WAVE DATA

In order to better account for the stochastic effects of the ship roll response under irregular wave conditions, the data from the irregular wave case are used to train the SVM model. In this case, the overall hydrodynamic moment in equation (12) also includes contributions from the incident wave exciting force. Therefore, the total wave force may be decomposed as follows.

$$\begin{aligned} F_h(t) = & -A_\infty \ddot{\xi}(t) - \int_{-\infty}^{t} K_r(t-\tau)\,\dot{\xi}(\tau)\,\mathrm{d}\tau \\ & - C\xi(t) + F_{ex,l}(t) + F_{h,r}(t) \end{aligned} \tag{15}$$

where, A_∞ is the infinite frequency added mass, C is the hydrostatic restoring coefficient, $K_r(t)$ is the radiation impulse response function kernel and $F_{ex,l}(t)$ is the linear incident wave exciting force, which includes the Froude-Krylov and diffraction components. The radiation impulse kernel and linear incident wave force can be easily derived from linear potential flow theory. Therefore, the residual nonlinear force can be expressed as:

$$\begin{aligned} F_{h,r}(t) = & F_h(t) + A_\infty \ddot{\xi}(t) + \int_{-\infty}^{t} K_r(t-\tau)\,\dot{\xi}(\tau)\,\mathrm{d}\tau \\ & + C\xi(t) + F_{ex,l}(t) \end{aligned} \tag{16}$$

The nonlinear residual force under stochastic wave conditions results from nonlinear wave-structure interactions and viscous effects. The features used in the SVM model are time-lagged records of wave elevations and ship roll velocities. The choice to include future values of the incident wave elevation is guided by the non-causal horizon of the linear potential flow impulse response function of the incident wave excitation force. When simulations or experiments are used to train the LS-SVM model, the past and future records of the wave elevations are known. The non-causal dependence on the incident wave elevation does not impose practical limits to subsequent simulation, as it may be pre-computed in the absence of the body.

It is assumed the most pertinent feature in a nonlinear ship roll damping model is the relative flow velocity around the hull and in the vicinity of the bilge keels. Therefore, the records of the ambient irregular wave elevations and ship velocities are included in the input features of the SVM nonlinear residual hydrodynamic force model $y_i = F_{h,r}(t_i)$, while the displacement and acceleration dependence is accounted for in the conventional linear terms in Eq. (15).

In the context of the LS-SVM model described by Eqs. (2)-(7), the training and test data samples $\{\boldsymbol{x}_i, y_i\}$ are defined as $\boldsymbol{x}_i = \left[\eta_{t_{i-d}}, \ldots, \eta_{t_{i-1}}, \eta_{t_i}, \eta_{t_{i+1}}, \ldots, \eta_{t_{i+d}}, \dot{\xi}_{t_i}, \dot{\xi}_{t_{i-1}}, \ldots, \dot{\xi}_{t_{i-d}}\right]$, and $y_i = F_{h,r}(t_i)$. Here, η is the incident wave elevations, and d is the duration of the past and future record that takes into account memory effects. In the present case, d is set to be 8 seconds as well.

The incident wave elevations, ship kinematics, total hydrodynamic force generated by the CFD simulation in irregular waves and the linear potential force components obtained from a potential flow panel method, are used to train the LS-SVM model. As in the case of the free-decay tests in calm water, part of the data is randomly selected as training samples and the rest are used for testing. The number of training samples used in the irregular wave cases was $N = 2000$. The hyperparameters are again optimized via cross-validation.

Two different kernels are considered in this section, the Gaussian and linear kernels. As stated in the previous section, the linear kernel may be viewed as a leading order linear approximation of the more general Gaussian kernel model. It may also be thought of as an equivalent linearization with memory. Moreover, the linear kernel may be converted into a frequency-domain transfer function, leading to a very efficient implementation in practice.

SVM REGRESSION MODEL WITH LINEAR KERNEL

Combining equations (12) and (15), the equation of motion in irregular waves can be expressed as:

$$\begin{aligned}(I+A_\infty)\ddot{\xi}(t)+\int_{-\infty}^{t}K_r(t-\tau)\,\dot{\xi}(\tau)\,\mathrm{d}\tau+C\xi(t)\\ =F_{ex,l}(t)+F_{h,r}(t)\end{aligned} \tag{17}$$

where, the nonlinear residual hydrodynamic force $F_{h,r}(t)$ is estimated by the LS-SVM regression model, and will be referred to as $F_{h,\text{lin-kernel}}$ in what follows.

Since the linear kernel takes the form

$$k(\boldsymbol{x},\boldsymbol{z}_i)=\boldsymbol{x}^{\mathsf{T}}\boldsymbol{z}_i \tag{18}$$

the estimated hydrodynamic force becomes

$$F_{\text{SVM,lin-kernel}}(t)=\sum_{i=1}^{N}\lambda_i\boldsymbol{x}^{\mathsf{T}}\boldsymbol{z}_i+b \tag{19}$$

where $\boldsymbol{z}_i=[z_{i,1},z_{i,2},\ldots,z_{i,p}]$ is the training sample containing p features.

Expanding $\boldsymbol{x}^{\mathsf{T}}\boldsymbol{z}_i=\sum x_j z_{ij}$ plugging in equation (19) and re-organizing terms, the LS-SVM model with a linear kernel may be expressed in the form:

$$F_{\text{SVM,lin-kernel}}(t)=\sum_{j=1}^{p}c_jx_j+b \tag{20}$$

where, p is the number of vector features $x_j, \quad j=1,2$. Here $p=2$, where $p=1$ corresponds to the input wave elevation record feature x_1 defined as the vector of time samples $\eta(t+\tau), \quad \tau=-T_c,\ldots,0,\ldots,T_c$, and $p=2$ corresponds to the roll velocity record feature x_2 defined as the vector of time samples, $\dot{\xi}(t+\tau), \quad \tau=-T_c,\ldots,0$.

Converting Eq. (20) into the frequency domain via the Fourier transform, and invoking the time-shift property:

$$\begin{aligned}x(t)&\rightarrow X(\omega)\\ x(t-\tau)&\rightarrow e^{-i\omega\tau}X(\omega)\end{aligned} \tag{21}$$

the estimated LS-SVM force in the frequency domain becomes:

$$\begin{aligned}&\mathbb{F}_{\text{SVM,lin-kernel}}(\omega)\\ &\quad=\mathbb{F}_{\text{SVM-}\eta}(\omega)H(\omega)+i\omega\mathbb{F}_{\text{SVM-v}}(\omega)\Xi(\omega)\end{aligned} \tag{22}$$

$H(\omega)$ is the Fourier transform of the wave elevation $\eta(t)$, and $\Xi(\omega)$ is the Fourier transform of the ship roll displacement $\xi(t)$.

Converting Eq. (17) into the frequency domain and plugging in Eq. (22), the equation of motion becomes:

$$\begin{aligned}&\left[-\omega^2(I+A_\infty)+i\omega\mathbb{K}_r(\omega)+C\right]\Xi(\omega)\\ &=\left[\mathbb{F}_{ex,l}(\omega)+\mathbb{F}_{\text{SVM-}\eta}\right]H(\omega)+i\omega\mathbb{F}_{\text{SVM-v}}(\omega)\Xi(\omega)\end{aligned} \tag{23}$$

Therefore, the transfer function of the roll displacement as a function of the incident wave elevations becomes:

$$\Xi(\omega)=\frac{\mathbb{F}_{\text{ex,l}}(\omega)+\mathbb{F}_{\text{SVM-}\eta}(\omega)}{-\omega^2(I+A_\infty)+i\omega\mathbb{K}_r(\omega)+C-i\omega\mathbb{F}_{\text{SVM-v}}(\omega)} \tag{24}$$

It is seen from equation (24) that the residual hydrodynamic force modeled by the linear LS-SVM kernel induces an excitation residual force transfer function which appears in the numerator and a damping coefficient which appears in the denominator. These effects are additive to the corresponding contributions from conventional linear potential flow theory. Moreover, they are both driven by nonlinear free surface and viscous separated flow physics contained in the CFD simulation record which is used to train the linear kernel LS-SVM machine learning model described in Eqs. (17)-(24).

Figure 6 illustrates a sketch of the training and testing results of the linear-kernel LS-SVM model. Figure 7 illustrates the comparison of the RAO transfer function derived using equation (24) and linear potential flow theory. The comparison shown in Figure 7 clearly illustrates that the LS-SVM force model introduces a significant damping effect.

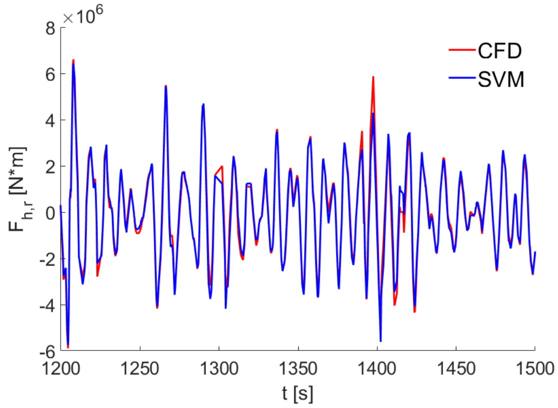

(a) Training data set

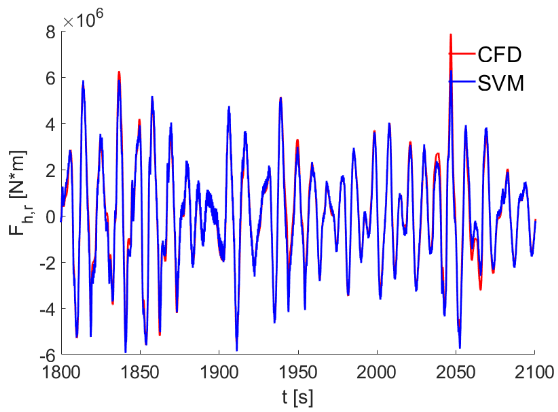

(b) Test data set

Figure 6: Hydrodynamic force residual prediction results using a linear kernel under irregular wave conditions

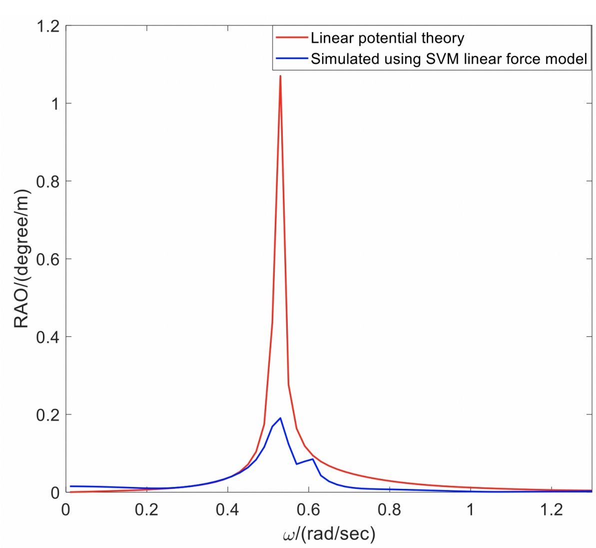

Figure 7: Comparison of the transfer function between linear potential flow heory and the linear-kernel LS-SVM model

The irregular wave spectral density used in the CFD simulation was next introduced in equation (24) to calculate the spectral density of the ship roll displacement. The resulting frequency domain roll response spectral density was then converted to time-domain records by invoking the inverse Fourier transform. Figure 8 illustrates the comparison of the ship roll displacement spectral densities obtained from the CFD time-domain simulation record and the linear-kernel LS-SVM frequency domain model. Furthermore, the difference of the standard deviation of the ship roll displacement was compared as well as a metric of the performance, since the standard deviation is a measure of the spectral energy. The difference of the standard deviation of the ship roll displacement between the two approaches is 9.54%.

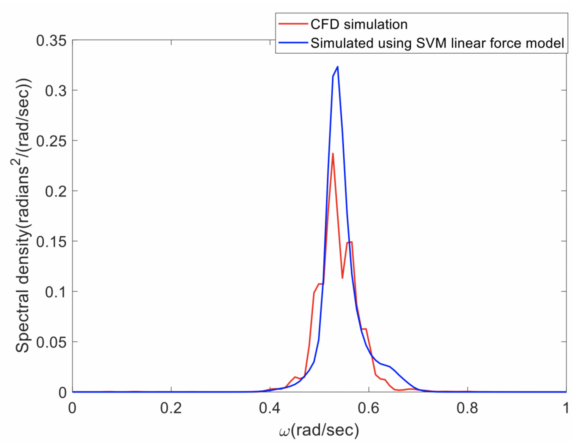

Figure 8: Comparison of spectral density of the ship roll displacement between the CFD simulation and the linear-kernel LS-SVM model

SVM REGRESSION MODEL WITH GAUSSIAN KERNEL

Having established the LS-SVM model using a linear kernel, we further explored the alternative of using Gaussian kernel trained against data from irregular wave records. The feature selection and SVM training process are the same as that for the linear kernel. The nonlinear residual force in Eq. (17) is estimated now by the SVM regression model with a Gaussian kernel. In what follows, the estimated nonlinear residual force in Eq. (17) is referred to as $F_{\mathrm{SVM,nl}}(t)$.

Since the Gaussian kernel [see Eq. (8)] is a nonlinear function of its arguments, the equation of motion cannot be converted into the frequency domain. In order to validate the feasibility of using the Gaussian-kernel-SVM model, Eq. (17) with the estimated nonlinear force $F_{\mathrm{SVM,nl}}(t)$ is simulated directly in the time-domain.

Figure 9 shows the training and test results of the hydrodynamic force obtained from the simulation of the Gaussian-kernel-SVM model. Figure 10 shows the spectral density of the ship kinematics estimated using the Gaussian-kernel-SVM model to generate time-domain records of the roll response. The difference of the standard deviation of the ship roll displacement obtained from the CFD simulations and the Gaussian SVM model is 5.67%.

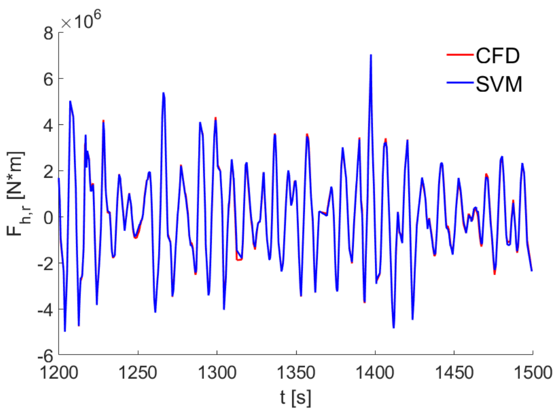

(a) Training data set

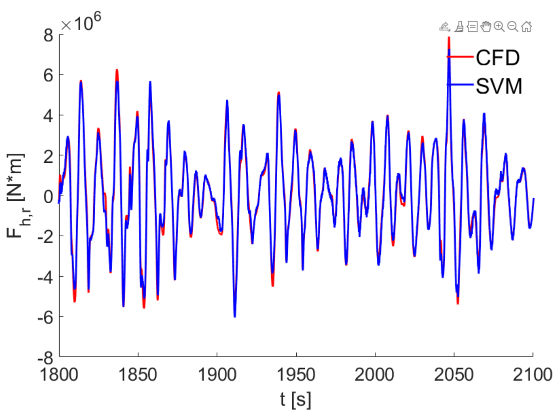

(b) Test data set

Figure 9: Hydrodynamic force residual prediction results using a linear Gaussian kernel under irregular wave conditions

It may be seen from Figures 8 and 10 that the SVM model using the nonlinear and the more general Gaussian kernel leads to an increased accuracy of the spectral density of the roll motion and better agreement with the results from the CFD simulations which are assumed to correctly capture all flow physics. Yet, the performance of the SVM model using the linear kernel is satisfactory and readily amenable for use in design practice using the efficient machinery of linear system theory. As such, it may be interpreted as an equivalent linearization with memory.

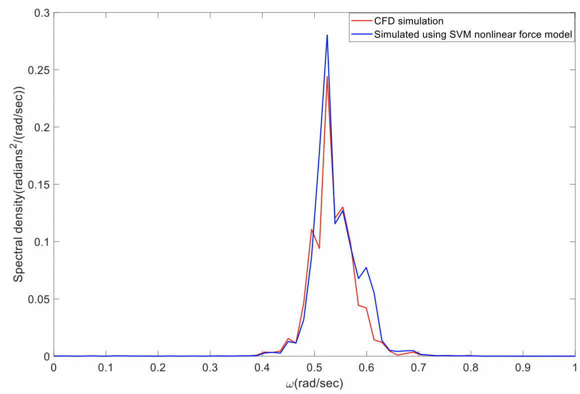

Figure 10: Comparison of spectral density of ship roll displacement between CFD simulation and the Gaussian-kernel-SVM model

DISCUSSION AND CONCLUSION

A series of simulations have been carried out for a rectangular barge with bilge keels using a 2D CFD solver. The CFD simulations are validated by comparing results of free decay and regular wave simulations with experiments.

Based upon the training data generated by validated CFD simulations, generalized SVM regression models are developed that establish the mapping between the dependent nonlinear roll hydrodynamic force and the input features. The wave elevation record and the ship roll velocity over a time window of finite duration are selected as the input features. The kernel of the SVM algorithm encodes the association between the features of the target samples to those of the training samples, and predicts the target value of the dependent quantity being modeled as a function of the kernel arguments which are the target and training features. By randomly selecting a set of training samples, the model was found to achieve a very good generalization capability to predict unseen targets via the training process.

In the context of ship roll hydrodynamics, when high-fidelity CFD simulation records of the ship roll hydrodynamics and motions in an irregular sea state are available, the SVM regression model establishes a general, efficient and accurate nonlinear model which provides a very good estimate of the nonlinear ship roll hydrodynamic loads in regular and irregular waves. Both the linear and nonlinear Gaussian kernels have been tested in the present paper. The Gaussian kernel has better accuracy and generalization capability to model the nonlinear force signal. However, the linear kernel enables the use of linear frequency domain analysis and renders its use more efficient in design practice.

Future work will be conducted to test the SVM model training in different sea states. The selection of a representative seastate will be investigated, allowing the training of the SVM once for subsequent use in the multitude of seastates needed in design practice, circumventing the need for time-consuming CFD simulations and experimental testing.

ACKNOWLEDGEMENTS

This work is supported by the U. S. Office of Naval Research (ONR) under Contract N00014-17-1-2985 monitored by Dr. Woei-Min Lin.

REFERENCES

Bassler, C. C. (2013) "Analysis and modeling of hydrodynamic components for ship roll motion in heavy weather," Virginia Tech Doctoral Dissertation.

Bishop, C. M. (2006) Pattern Recognition and Machine Learning, Springer.

Christianini, N. and Swane-Taylor, J. (2000) An Introduction to Support Vector Machines and Other Kernel-based Learning Methods. Cambridge University Press.

Falzarano, J., Somayajula, A., and Seah, R. (2015) "An overview of the prediction methods for roll damping of ships," Ocean Systems Engineering, Vol. 5, No. 2, pp. 55-76.

Fasshauer, G. E., and McCourt, M. J. (2012) "Stable Evaluation of Gaussian Radial Basis Function Interpolants," SIAM Journal on Scientific Computing, Vol. 34, Issue 2, pp. 737-762.

Irkal, M. A. R., Nallayarasu, S., and Bhattacharyya, S. K. (2014) "Experimental and CFD simulation of roll motion of ship with bilge keel," Proceedings of the RINA International Conference on Computational and Experimental Marine Hydrodynamics, 3-4 December, Chennai, India. Vol. 2, pp. 157-166

Irkal, M. A. R., Nallayarasu, S., and Bhattacharyya, S. K. (2016) "CFD approach to roll damping of ship with bilge keel with experimental validation," Applied Ocean Research, Vol. 55, No. C, pp. 1-17.

Kianejad, S. S., Enshaei, H., Duffy, J., Ansarifard, N., and Ranmuthugala, D. (2019) "Ship roll damping coefficient prediction using CFD" Journal of Ship Research, Vol. 63, No. 2, pp. 108-122.

Luo, W., Soares, C. G., and Zou, Z. (2016) "Parameter identification of ship maneuvering model based on support vector machines and particle swarm optimization," Journal of Offshore Mechanics and Arctic Engineering, Vol. 138, Issue 3: 031101.

Nocedal J. and Wright S. J. (2006) Numerical Optimization, Springer.

Sclavounos, P. D., and Ma, Y. (2018) "Artificial Intelligence Machine Learning in Marine Hydrodynamics," Proceedings of the ASME 37th International Conference on Ocean, Offshore and Arctic Engineering,17-22 June, Madrid, Spain.

Siemens PLM Software (2019). Simcenter STAR-CCM+ User Guide Version 2019.1. Siemens Product Lifecycle Management Software Inc.

Suykens, J. A. and Vandewalle, J. (1999) "Least squares support vector machine classifiers," Neural Processing Letters, Vol. 9, No. 3, pp. 293-300.

Wassermann, S., Feder, D. F., and Abdel-Maksoud, M. (2016) "Estimation of ship roll damping—A comparison of the decay and the harmonic excited roll motion technique for a post-Panamaz container ship," Ocean Engineering, Vol. 120, pp. 371-382.